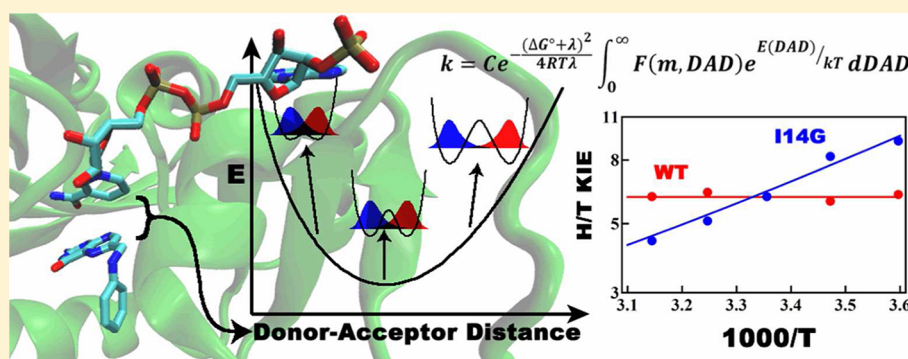


Hydrogen Donor–Acceptor Fluctuations from Kinetic Isotope Effects: A Phenomenological Model

Daniel Roston, Christopher M. Cheatum, and Amnon Kohen*

Department of Chemistry, University of Iowa, Iowa City, Iowa 52242, United States

S Supporting Information



ABSTRACT: Kinetic isotope effects (KIEs) and their temperature dependence can probe the structural and dynamic nature of enzyme-catalyzed proton or hydride transfers. The molecular interpretation of their temperature dependence requires expensive and specialized quantum mechanics/molecular mechanics (QM/MM) calculations to provide a quantitative molecular understanding. Currently available phenomenological models use a nonadiabatic assumption that is not appropriate for most hydride and proton-transfer reactions, while others require more parameters than the experimental data justify. Here we propose a phenomenological interpretation of KIEs based on a simple method to quantitatively link the size and temperature dependence of KIEs to a conformational distribution of the catalyzed reaction. This model assumes adiabatic hydrogen tunneling, and by fitting experimental KIE data, the model yields a population distribution for fluctuations of the distance between donor and acceptor atoms. Fits to data from a variety of proton and hydride transfers catalyzed by enzymes and their mutants, as well as nonenzymatic reactions, reveal that steeply temperature-dependent KIEs indicate the presence of at least two distinct conformational populations, each with different kinetic behaviors. We present the results of these calculations for several published cases and discuss how the predictions of the calculations might be experimentally tested. This analysis does not replace molecular QM/MM investigations, but it provides a fast and accessible way to quantitatively interpret KIEs in the context of a Marcus-like model.

The detailed mechanisms of enzyme-catalyzed H-transfer reactions have tantalized researchers for many years, because of the important intellectual questions and medicinal applications associated with enzymes. It is now well accepted that both enzyme-catalyzed and nonenzymatic hydrogen transfers involve quantum mechanical tunneling, the phenomenon by which a particle passes through an energy barrier due to its wavelike properties. Because tunneling is highly mass dependent, kinetic isotope effects (KIEs) are excellent probes of these reactions. In recent years, the temperature dependence of KIEs has emerged as an important indication of the nature of tunneling and has suggested that fluctuations of the donor–acceptor distance (DAD) may be mechanistically important.^{1–9} Here the DAD is defined as the distance between the two heavy atoms transferring the hydrogen.

Conventional transition state theory (TST) models chemical kinetics under a set of assumptions where the width of the barrier is unimportant; all that affects the rate is the height of

the barrier. Some attempts to account for the effects of tunneling on KIEs rely on corrections to TST of the form

$$\text{KIE} = \frac{k_L}{k_H} = \frac{Q_L k_L^{\text{TST}}}{Q_H k_H^{\text{TST}}} \quad (1)$$

where k^{TST} is the TST rate for the light (L) or heavy (H) isotope and Q is the correction for tunneling effects for each isotope. The tunneling correction is generally based on a parabolic barrier with some more sophisticated treatments available, but the barrier is assumed to be static.¹⁰ Tunneling corrections can reproduce both temperature-dependent and temperature-independent KIEs, but such simple corrections to TST cannot reproduce small and temperature-independent KIEs where the rate is temperature-dependent ($E_a > 0$). Certain

Received: May 9, 2012

Revised: August 1, 2012

Published: August 3, 2012

enzymatic, as well as nonenzymatic, reactions, however, exhibit just that: large activation energies, but temperature-independent KIEs that are not inflated.^{11–19} To account for this behavior, many researchers have adapted Marcus theory of electron tunneling²⁰ to the situation of hydrogen tunneling (Figure 1). The Marcus-like models^{6,8,21} (also known as full-

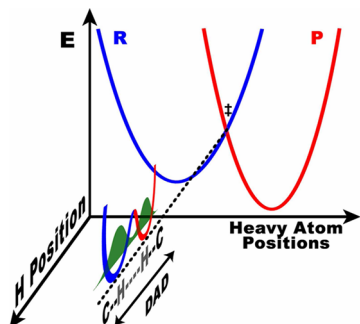


Figure 1. Marcus-like model of hydrogen tunneling. The heavy atoms reorganize to bring the reactant (blue) and product (red) potential surfaces to a point of transient degeneracy (\ddagger , the TRS) where the hydrogenic wave function (green) can pass from the donor well to the acceptor well, which is called tunneling. The TRS actually represents a seam in multidimensional space, including all conformations where the reactant and product surfaces are degenerate. Figure 2 highlights how the fluctuation of the DAD along this seam dictates the probability of tunneling at the TRS.

tunneling models,²² environmentally coupled tunneling,¹ and vibrationally enhanced tunneling⁵) suggest that heavy-atom motions bring the system to a tunneling-ready state (TRS), where the vibrational energy levels for the hydrogen in the reactant and product states are degenerate and tunneling can occur.^{1,2,8,9,23–28} This type of model gives a rate constant (k) with the functional form

$$k = \frac{|V|^2}{\hbar} \sqrt{\frac{\pi}{\lambda k_B T}} e^{-(\Delta G^\circ + \lambda)^2 / 4k_B T \lambda} \int_0^\infty F(m, \text{DAD}) e^{E(\text{DAD})/k_B T} d\text{DAD} \quad (2)$$

In this equation, the factors in front of the integral include the electronic coupling between the reactants and products (V) and the thermally averaged equilibrium probability of heavy-atom “reorganization” to reach the TRS, which depends on the reaction driving force (ΔG°), the reorganization energy (λ), and the absolute temperature (T); k_B is Boltzmann’s constant. These factors are nearly completely insensitive to the mass of the transferred particle, so only the integral contributes to the isotope effects. The integral computes the probability of tunneling to form products once the system reaches the TRS. The first factor inside the integral gives the probability of tunneling as a function of the mass (m) of the transferred particle (H, D, or T) and the DAD. The second factor in the integral is a Boltzmann factor giving the probability of being at any given DAD. Thus, because the thermal reorganization to reach the TRS is isotopically insensitive, but tunneling at the TRS is isotopically sensitive, the model accounts for either temperature-dependent or temperature-independent rates with temperature-dependent or temperature-independent KIEs. Previous studies have reported all four possibilities for both enzymatic and nonenzymatic systems, requiring a flexible model that can accommodate all of these outcomes. We note that this kind of model assumes that all the motions of the

system are in thermal equilibrium with the environment, in accordance with established theories.^{3,9,23,29,30}

Interestingly, several enzymes that exhibit temperature-independent KIEs have mutants for which KIEs are temperature-dependent. Qualitative arguments have rationalized that differences in thermal fluctuations of the DAD (the Boltzmann factor in the integral of eq 2) can account for both behaviors (Figure 2).^{1,8} In the case of temperature-dependent KIEs,

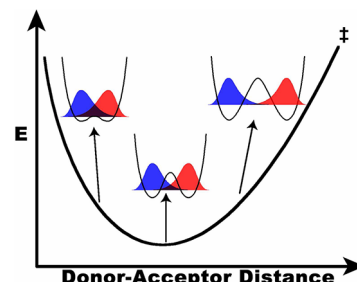


Figure 2. PES of the DAD coordinate along the seam where the reactant and product surfaces are degenerate (the TRS). Slices along the orthogonal tunneling coordinate are shown at three different DADs, demonstrating the change in overlap between reactant (blue) and product (red) wave functions. The wave function overlap at each distance is proportional to the tunneling probability at that distance and is isotopically sensitive. This model uses the temperature dependence of KIEs to determine the population distribution of DADs, which is dictated by this PES.

thermal excitations that populate conformations with shorter DADs, where the heavy isotope can tunnel, will lower the KIE as the temperature increases. In contrast, if the enzyme stabilizes a TRS with a very short DAD, where tunneling is efficient for both isotopes, then thermal activation will not alter the magnitude of the KIE.³¹ Although this model appears to account for the wide range of experimental observations, few attempts have tried to quantitatively link the size and temperature dependence of KIEs to the population distribution along the DAD coordinate,^{14,24,32} and in most cases, detailed QM/MM simulations have been necessary to achieve a molecular understanding of the reaction.^{26,33–35}

To assist experimentalists in quantitative analysis of data, we expand on previous efforts to connect the temperature dependence of KIEs to a simple physical model. The value of such a phenomenological model, like that of most statistical models, is that it captures the essential physics of the problem for initial assessment of the system under study without all of the molecular detail of an explicit simulation. Although cases where a detailed molecular interpretation is required to understand the chemistry motivate high-level simulations, e.g., QM/MM, they are not necessary in many situations where an analysis using modified TST or Marcus-like models provides sufficient physical insight into the reaction dynamics (including assessment of whether molecular simulation is needed). We apply the proposed model to several different enzymes and their mutants, including dihydrofolate reductase (DHFR),^{12,36–39} morphinone reductase (MR),¹⁴ thymidylate synthase (TSase),^{13,40} alcohol dehydrogenase (ADH),^{11,41} formate dehydrogenase (FDH),⁴² and pentaerythritol tetranitrate reductase (PETNR),¹⁵ as well as two nonenzymatic sigmatropic rearrangements.^{17,43} In contrast to some previous fitting models, we maintain that the experimental data correspond to a single-exponential relationship, and thus, any

fitting model must be limited to two adjustable parameters. The question for the experimentalist trying to interpret data is what physical quantities those parameters represent. Fits to the Arrhenius equation and the parameters of that equation have limited physical meaning (i.e., ΔE_a and A_H/A_D) for these kinds of reactions. The method described here allows experimental enzymologists and organic chemists to obtain a quantitative interpretation of their results in terms of a distribution of DADs, but without requiring the expertise, time, and resources necessary to conduct costly QM/MM simulations.^{3–5,26,33–35,44–48} Furthermore, these calculations result in a number of intriguing predictions that could be examined experimentally.

METHODS

We conducted all geometry optimizations and potential-energy surface (PES) scans at the B3LYP/6-31+G* level with Gaussian 03.⁴⁹ We did all other calculations with Mathematica 7.⁵⁰

The overall framework used here follows the model developed by Kuznetsov and Ulstrup (ref 23, eq 2), but with significant modifications relative to other attempts to implement this type of model.^{14,24,32,51} Because the factors outside the integral of eq 2 are essentially isotopically insensitive (i.e., affected by motions of many heavy atoms with little or no contribution of the isotopically labeled atom), the following ratio of integrals contains the experimental primary KIEs:

$$\text{KIE} = \frac{k_L}{k_H} = \frac{\int_{r_1}^{r_2} F(m_L, \text{DAD}) e^{E(\text{DAD})/kT} d\text{DAD}}{\int_{r_1}^{r_2} F(m_H, \text{DAD}) e^{E(\text{DAD})/kT} d\text{DAD}} \quad (3)$$

As mentioned above, the first factor in each integral represents the probability of tunneling as a function of the DAD and the mass of the transferred particle and the second factor is a Boltzmann factor, giving the probability of being at any given DAD. The integral is formally over all DADs, but in reality, it is negligible outside of a small region within which the DAD is short enough to give a non-zero tunneling probability ($\text{DAD} < r_2$) but long enough that van der Waals repulsions between the donor and acceptor are small ($\text{DAD} > r_1$). Because upon calculation of KIEs many of the assumptions and expressions that are not isotopically sensitive drop from the equation, and because many experiments directly measure KIEs, without measuring individual rates,²¹ this equation should have greater utility than individual rate equations.

Tunneling Probability. Previous calculations of this type have based the tunneling probability on nonadiabatic models using harmonic^{24,51} or Morse^{14,32} potentials to describe the donor and acceptor wells. For many reactions, though, adiabatic coupling is very important.⁵² Thus, we allow for strong coupling between the donor and acceptor wells, which is more relevant to hydride and proton transfers and gives markedly different results (see below). As with previous models, we assume that the probability of tunneling as a function of DAD does not differ among similar reactions. For computational simplicity, therefore, we base our calculations on the hypothetical symmetric transfer of H^- from reduced to oxidized nicotinamide moieties, in a manner similar to a model for symmetric H-transfer in solution.⁵³ The donor and acceptor moieties are analogous to the ubiquitous nicotinamide biological cofactor NAD(P)^+ . A hydrogen truncates the nicotinamide rings where they normally link to the ribosyl

moiety of NAD(P)^+ , so the system contains a total of 33 atoms (Figure 3) and an overall charge of +1. Heavy-atom geometries

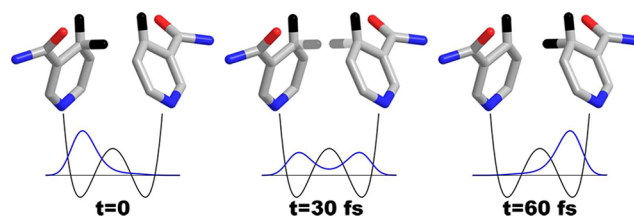


Figure 3. Time evolution of the ^1H wave function tunneling between two NAD^+ moieties frozen with a DAD of 3.2 Å. All the heavy atoms used in the calculations are shown, along with hydrogens of particular interest. When the system reaches the TRS ($t = 0$), the hydrogen is effectively localized in the donor well, but its probability density evolves over time, as shown. The coherent oscillation of this wave packet dephases because of environmental perturbations, yielding some finite probability of decaying to the acceptor state, resulting in net transfer. An exponential decay with a time constant of 10 fs models the dephasing, which is consistent with more sophisticated calculations.^{57–59}

of the two nicotinamide moieties are optimized at a range of DADs from 2.6 to 3.5 Å with the C–H–C angle constrained at 180° and the hydrogen at the midpoint between the donor and acceptor C4 atoms. We previously found this approach sufficient for assessment of the structure of the TRS in yeast ADH.⁵⁴ At each DAD, we scanned the PES for linear hydrogen transfer with all other atoms frozen and fit these scans (least-squares) to symmetric quartic potentials (Figure 4).

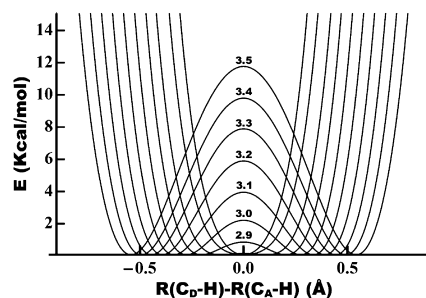


Figure 4. PESs for linear $\text{C-H} \rightarrow \text{C}$ transfer between two NAD^+ moieties with the heavy atoms frozen at a range of DADs (defined as the distance from C4 of the donor to C4 of the acceptor). Each surface is a symmetric quartic fit (least-squares) to a scan of 15–25 points (depending on the DAD) calculated at the B3LYP/6-31+G* level. The DAD in angstroms is labeled above the barrier for each surface. From this figure, it is clear that below 2.8 Å there is no barrier to H-transfer and calculations of ZPE indicate that the hydrogen is above the barrier at even longer distances, depending on the isotope (cf. Figure 5).

When the system reaches the TRS, the hydrogen is localized in the donor well. Before the degeneracy of the TRS is broken, the donor wave function evolves so that some probability density ends up in the acceptor well (Figure 3). To calculate the time evolution of the probability density, we construct donor and acceptor wave functions for each isotope from linear combinations of the ground (φ_0) and first excited (φ_1) eigenstates of the potentials in Figure 4.

$$\Psi_{\text{donor}} = \frac{1}{\sqrt{2}} \varphi_0 + \frac{1}{\sqrt{2}} \varphi_1 \quad (4)$$

$$\Psi_{\text{acceptor}} = \frac{1}{\sqrt{2}}\varphi_0 - \frac{1}{\sqrt{2}}\varphi_1 \quad (5)$$

When the system reaches the TRS, the nonstationary donor wave function evolves in time by coherent oscillations between the donor and acceptor state with a period (τ) dependent on the tunneling splitting (ΔE_t),⁵⁵ where

$$\tau(m, \text{DAD}) = \frac{\hbar}{\Delta E_t} \quad (6)$$

and ΔE_t is the difference in energy between φ_0 and φ_1 :

$$\Delta E_t = E(\varphi_1) - E(\varphi_0) \quad (7)$$

We calculate ΔE_t for each DAD for H, D, and T by numerical solution of the Schrödinger equation as described previously.⁵⁴ To obtain an expression for ΔE_t as a function of DAD, we fit (least-log-squares) the calculated values to a sum of two exponentials, which correspond to the behaviors above and below the barrier (Figure 5). When the zero-point energy

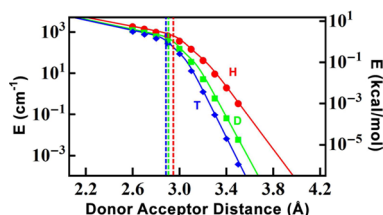


Figure 5. Tunnel splitting (ΔE_t) of the three isotopes of hydrogen as a function of DAD (eq 7), calculated as the difference in energy of the first two eigenstates of the potentials in Figure 4. The vertical lines indicate the DAD at which each isotope's ZPE is greater than the height of the reaction barrier.

(ZPE) of the hydrogen is above the barrier, the process is not formally tunneling, but an advantage of this methodology is that the calculations smoothly transition between the region of tunneling²⁷ and the region of over-the-barrier events.⁵⁶

The oscillations of the hydrogen wave function result in a probability density in the acceptor well (corresponding to net transfer) as a function of time (t) after reaching the TRS given by the expression

$$P(t, m, \text{DAD}) = -\frac{1}{2} \left[1 + \cos \left(\frac{2\pi}{\tau(m, \text{DAD})} t \right) \right] \quad (8)$$

After reaching the TRS, however, environmental perturbations lead to dephasing of the coherent wave function, such that the oscillations effectively cease after a short dephasing time. Calculating the rate of dephasing is not within the scope of this model, but we can approximate the rate as an exponential decay with a time constant (θ) of 10 fs.⁵⁷ This approximation is consistent with other treatments that calculated the decay of the probability flux correlation function based on the spectral density of the environment,^{58,59} a method first described for solution reactions⁶⁰ that has found much subsequent use in solution and enzymes.^{25,61} Furthermore, the general behavior of the model is not sensitive to the value of θ within the range of 1–100 fs. Using this exponential dephasing, the overall probability of tunneling as a function of DAD (Figure 6) is

$$F(m, \text{DAD}) = \frac{\int_0^\infty e^{(t/\theta)} \times P(t, m, \text{DAD}) dt}{\int_0^\infty e^{(t/\theta)} dt} \quad (9)$$

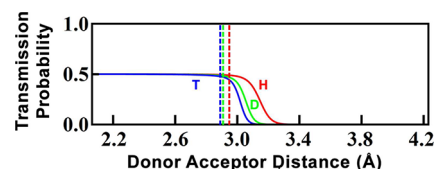


Figure 6. Transmission probability for each of the three isotopes of hydrogen as a function of DAD (eq 9). The vertical lines indicate the DAD at which each isotope's ZPE is greater than the height of the reaction barrier.

We expect this term to be nearly invariant among different hydride transfers between carbon atoms, and at least to yield reasonable trends for other types of hydride and proton transfers. The utility of this function for several different reactions is explored below.

DAD Population Distribution. In eq 3, the Boltzmann factor within the integral represents the population distribution along the DAD coordinate. This term dictates the size and temperature dependence of the KIEs. We analyze experimental data that range from reactions with completely temperature-independent KIEs (within experimental error) to reactions with steeply temperature-dependent KIEs. Most surprisingly, we find that a model with a single population could not fit the steeply temperature-dependent KIEs. Thus, we present two models below: a single-population model for KIEs with little or no temperature dependence and a model with two populations that accounts for KIEs with all levels of temperature dependence. We use these two forms of the Boltzmann factor in eq 3 to fit the KIEs. Importantly, we use only two parameters to fit the data with either model. Because experiments measure the temperature dependence of KIEs across a narrow temperature range, and this dependence follows a single-exponential relationship, at most two fitting parameters are justified.

Temperature-Independent KIEs: One Population.

Previous methods used a harmonic potential to approximate the PES that describes the DAD coordinate,^{14,24,32,33,51} and where possible, we follow this standard. This gives a Gaussian population distribution of the form

$$e^{E(\text{DAD})/k_B T} = e^{f(\text{DAD} - \text{DAD}_0)^2/k_B T} \quad (10)$$

where the average DAD (DAD_0) and the force constant (f) of the corresponding harmonic potential are adjustable fitting parameters when this factor is substituted into eq 3. In formal terms, this distribution is normalized, but because the probability distribution of DADs is not mass-sensitive, the normalization constants for the two isotopes are equal and thus cancel one another. This type of distribution can fit KIEs with little to no temperature dependence, but even if we allow for physically unreasonable parameters, this distribution cannot lead to the small, steeply temperature-dependent KIEs observed in some reactions (Figure S1 of the Supporting Information).

Temperature-Dependent KIEs: Two Populations.

It is not surprising that simple distributions like eq 10 fail in some cases. For reactions where the donor and acceptor are not well constrained in reactive orientations, they are unlikely to have

the same steep potential-energy gradient at long separations (when held by “soft” protein or solvent forces) as when closely approaching each other (under van der Waals radii), as implied by a harmonic potential. Our efforts to fit the temperature-dependent KIEs with more sophisticated functions lead to the conclusion that at least two distinct populations are required to fit these experimental data in the context of a Marcus-like model.

After exploring a number of ways to describe the population distribution in systems with steeply temperature-dependent KIEs, we find that the following is the simplest model that can fit the data. One population is centered at a short enough DAD ($\text{DAD}_{\text{short}}$) that all isotopes cross the dividing surface between the reactant and product with similar probabilities (i.e., the KIE is unity for this population). We choose this population as the zero of free energy ($G = 0$) for the sake of computational simplicity. A second, lower-energy population is centered at a longer DAD (DAD_{long}), where the overall tunneling probability is lower but the isotope effect is larger. In this model, the precise DAD of the shorter population does not significantly affect the fit to the data, as long as the DAD is short enough that the ZPEs of all three isotopes are above the reaction barrier (cf. vertical lines in Figure 6). This population effectively corresponds to a semiclassical transition state.^{34,62,63} We assume that the two conformational populations are in thermal equilibrium with one another and that the temperature-dependent change in the relative populations gives rise to the temperature dependence of the KIEs. Thus, the population distribution (the Boltzmann factor in eq 3) has the form

$$e^{-E(\text{DAD})/k_B T} = \delta(\text{DAD} - \text{DAD}_{\text{short}}) + e^{-\Delta G/k_B T} \delta(\text{DAD} - \text{DAD}_{\text{long}}) \quad (11)$$

where the two fitting parameters are DAD_{long} (the DAD of the population at longer distances) and ΔG (the difference in free energy between the two populations). Including a distribution about the average DADs of the two populations requires more parameters and does not yield a better fit, so we leave the populations as δ functions. As with eq 10, this distribution function need not be normalized to calculate KIEs.

Fitting the KIEs. We fit (least-squares) experimental KIEs as a function of temperature to eq 3, using both the single-Gaussian distribution (eq 10) and the two-population distribution (eq 11). Except in cases where one attempts to fit steeply temperature-dependent KIEs to a single population, the fits converge to 16-digit precision within a few seconds, using a Sony laptop with an Intel Core2Duo P8700 processor (2.53 GHz) and 8 GB of RAM. A Mathematica for conducting this type of fitting is available free of charge on the web at <http://chemmath.chem.uiowa.edu/webMathematica/kohen/marcuslikemodel.html>.

RESULTS AND DISCUSSION

We propose a simple phenomenological model that allows quantitative fitting of experimental KIEs and their temperature dependence, yielding up to two physically meaningful parameters that describe the distribution(s) of DADs. To do so, we have modeled the tunneling probability, assuming adiabatic coupling between the donor and acceptor wells. This approach expands the space of possible reactions that can be modeled beyond those in which strictly nonadiabatic tunneling is appropriate.^{24,32} Several studies have provided in-depth analyses of the differences between adiabatic and nonadiabatic approaches in this type of vibronic model.^{52,64} Here, we find

that the coupling of the donor and acceptor increases the length of the C–H bond and substantially decreases the height of the barrier, yielding large regions of wave function overlap at DADs where nonadiabatic models predict negligible probabilities of tunneling (Figure 7). As a result, our adiabatic model

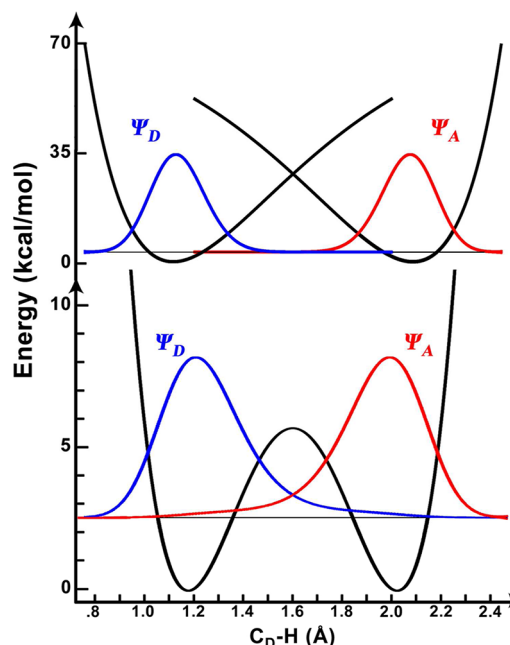


Figure 7. Comparison of the wave function overlap between donor (blue) and acceptor (red) states of ^1H for the nonadiabatic limit, using Morse potentials (top), and the adiabatic limit used in our calculations (bottom). In both examples, the DAD is set at 3.2 Å. The Morse wave functions are the ground eigenstates of the Hamiltonian, and the wave functions for the double-well potential were constructed as linear combinations of the ground and first excited eigenstates of the Hamiltonian.

demonstrates that tunneling occurs from DADs relatively close to the van der Waals distance of the two heavy atoms (3.4 Å for carbon). While several high-level simulations suggest tunneling from DADs between 2.6 and 2.8 Å,^{34,63} we have shown that there is no barrier to H-transfer at that distance (Figure 4) and that distance actually corresponds to the semiclassical transition state. Tunneling from longer DADs, however, is consistent with a model of the TRS of yeast ADH based on secondary KIEs⁵⁴ as well as high-level QM/MM simulations of DHFR.²⁶ A further advantage of this method is that we need not assume that every reactive trajectory occurs by tunneling. The transferred hydrogen in this model behaves as a quantum particle, regardless of the electrostatic environment applied by the heavy atoms of the system. Whether above or below the barrier, the hydrogen is wavelike.⁵⁶ Thus, as shown in Figure 6, the transmission probability smoothly transitions between DADs where the ZPE is below the barrier to those where it exceeds the barrier height. Even for these over-the-barrier trajectories, though, the heavy-atom reorganization remains the primary motion leading to H-transfer^{65,66} (i.e., “the reaction coordinate is the solvent coordinate”⁵⁶). In this type of mechanism, all isotopes cross the dividing surface to products with similar probability once they are above the barrier. As discussed below, this result turns out to be of vital importance in describing steeply temperature-dependent KIEs.

Table 1. Experimental ΔE_a Values and Resulting Fitting Parameters for the Systems Studied Here

enzyme/reaction			mutation/conditions/reactants			ΔE_a^a			fitting parameters		ref		
									one population			two populations	
									DAD ₀ ^b	f^c		DAD _{long} ^b	ΔG^d
DHFR active site mutants	WT	−0.1 ± 0.2	3.058	>250	3.057	>2.5	12						
	I14V	0.30 ± 0.07	3.082	200	3.064	2.3	67						
	I14A	0.38 ± 0.03	3.093	190	3.072	2.4	39						
	I14G	3.31 ± 0.07	NA ^e	NA ^e	3.307	3.8	67						
DHFR distal mutants	WT	−0.1 ± 0.2	3.058	>250	3.057	>2.5	12						
	G121V	0.25 ± 0.02	3.084	390	3.072	2.8	36						
	M42W	0.55 ± 0.03	3.119	80	3.072	1.9	37						
	G121V/M42W	3.7 ± 0.2	NA ^e	NA ^e	3.342	4.4	38						
bsADH ^f	WT > 30°	0.1 ± 0.2	3.094	>100	3.086	>2.0	11						
	WT < 30°	0.7 ± 0.2	NA ^e	NA ^e	3.158	1.1	11						
	L176V > 30°	1.7 ± 0.9	NA ^e	NA ^e	3.232	2.3	41						
	L176V < 30°	2.3 ± 0.5	NA ^e	NA ^e	3.282	3.1	41						
	L176A > 30°	1.6 ± 0.5	NA ^e	NA ^e	3.231	2.3	41						
	L176A < 30°	0.8 ± 0.6	NA ^e	NA ^e	3.158	1.3	41						
	L176G > 30°	1.4 ± 0.5	NA ^e	NA ^e	3.212	1.9	41						
	L176G < 30°	1.0 ± 0.7	NA ^e	NA ^e	3.177	1.4	41						
	L176Δ > 30°	1.8 ± 0.3	NA ^e	NA ^e	3.244	2.5	41						
	L176Δ < 30° ^g	−0.4 ± 0.3	3.095	>1000	3.094	>4.0	41						
	V260A > 40°	1.8 ± 0.7	NA ^e	NA ^e	3.239	2.4	41						
	V260A < 40°	0.0 ± 0.4	3.094	>100	3.091	>2.0	41						
MR ^f	W106A	0.0 ± 0.4	3.110	>150	3.110	>2.5	14						
	WT	2.0 ± 0.4	NA ^e	NA ^e	3.211	2.3	14						
	V108L	2.1 ± 0.4	NA ^e	NA ^e	3.235	2.6	14						
	NADH	0.1 ± 0.2	3.120	>400	3.117	>3	15						
PETNR ^f	NADPH	1.4 ± 0.1	NA ^e	NA ^e	3.175	1.9	15						
	TSase	H [−] transfer	0.0 ± 0.6	3.062	>100	3.061	>2	13					
FDH	H ⁺ transfer	8.3 ± 0.3	NA ^e	NA ^e	3.612	9.5	40						
	WT	−0.03 ± 0.04	3.057	>1000	3.056	>3	42						
[1,5]sigmatropic rearrangement ^f	pentadiene ^h	1.4	3.553	16	3.145	2.3	43						
	quinolizine	−0.01 ± 0.02	3.101	>2000	3.100	>5	17						

^aH/T KIEs except where noted. All energies are in kilocalories per mole. In some cases, raw data were not published so we used approximations of the actual data points and errors based on visual inspection of published figures (on log scales) in the fittings. Thus, the ΔE_a shown here may differ from previously published values but corresponds to the data points used in the modeling. ^bIn angstroms. Errors are <5% of the reported value. ^cIn kilocalories per mole per square angstrom. Only a lower bound is given for systems within error of $\Delta E_a = 0$; the lower bound is the value such that the calculated ΔE_a (in the middle of the observed temperature range, using the best fit value for DAD_0) is equal to the upper error of the observed ΔE_a ($\Delta E_a + \sigma$). Errors for other systems are <15% of the reported value. ^dOnly a lower bound is given for systems within error of $\Delta E_a = 0$; errors for other systems are <15% of the reported value. ^eNot applicable (NA) for systems with a ΔE_a of >1 kcal/mol at 298 K. ^fH/D KIEs. ^gThis model is not designed to fit inverse temperature dependence ($\Delta E_a < 0$). ^hErrors unavailable because individual data points were not published; measurements were taken at >450 K, so the one population model was successful despite a ΔE_a of >1 kcal/mol.

Our approach also expands the range of temperature dependencies of KIEs that can be quantitatively interpreted by a full-tunneling model. The previous phenomenological methods, which used only single harmonic potentials to describe the DAD coordinate, cannot reproduce the steep temperature dependence of KIEs that has been observed in a number of systems (see the Supporting Information). By allowing for two populations along the DAD coordinate, this model fits a variety of KIEs that have been reported for biological hydride and proton transfers, as well as nonenzymatic H-transfers (see examples below). As discussed in Methods, the nature of the experimental data (KIEs over a narrow temperature range, which conform to a single exponential) allows for at most two meaningful fitting parameters.

Fitting the KIEs. This method gives good fits to experimental KIEs exhibiting a wide range of temperature dependences (ΔE_a), resulting in physically meaningful population distributions along the DAD coordinate in a variety

of reactions. The fitted parameters for each reaction are listed in Table 1. The experimental data are from measurements by a number of independent researchers who used an assortment of techniques, and all cases represent intrinsic KIEs that are not masked by kinetic complexity. To give a sense of the quality of the fits, we present the results for the enzyme DHFR and two series of mutants in Figure 8.^{38,39,67} The model achieves similar accuracy for the other systems we examine (see details and figures in the Supporting Information): the nicotinamide-dependent C–H → C transfers in thermophilic ADH from *Bacillus stearothermophilus*, bsADH,^{11,41} and FDH,⁴² the C–H → N transfer between flavin and nicotinamide in two flavoenzymes, MR¹⁴ and PETNR,¹⁵ the hydride (C–H → C) and proton (C–H → O) transfers that are part of the kinetic cascade in TSase,^{13,40} and two nonenzymatic [1,5]sigmatropic rearrangements.^{17,43} Given the method of parametrizing the tunneling probability (eq 9), the details of this model are most applicable to C–H → C transfers involving nicotinamide

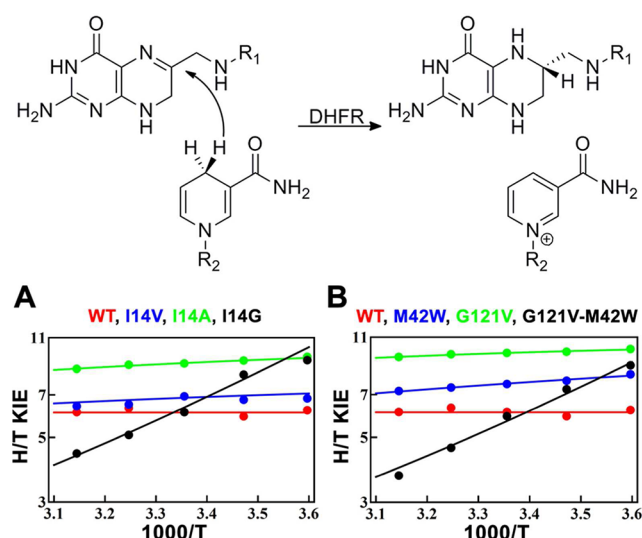


Figure 8. Reaction catalyzed by DHFR and the fits to KIEs from a series of active-site mutants (A) and a series of distal mutants (B). All fits correspond to the two-population model. Experimental data are from refs 38, 39, and 67.

cofactors (DHFR, bsADH, and FDH). One should interpret the precise results for the other three enzymes (MR, PETNR, and TSase) and the nonenzymatic reactions with caution, but we believe the overall trends among those reactions are fairly robust. To obtain more accurate results for those reactions, one could reparameterize the tunneling probability (eq 9) to focus on H-transfers more relevant to those systems.

We display the KIEs of Figure 8 (and those in the Supporting Information) as Arrhenius plots ($1/T$ vs KIE on a log scale), following the tradition of phenomenological analysis of KIEs by the Arrhenius or Eyring equations^{1,8}

$$\text{KIE} = \frac{k_L}{k_H} = \frac{A_L}{A_H} e^{\Delta E_a/kT} \quad (12)$$

where A_i is the Arrhenius pre-exponential factor for isotope i and ΔE_a is the difference in activation energy between the two isotopes. By this analysis, temperature-independent KIEs give a ΔE_a close to 0, often associated with an A_L/A_H greater than the semiclassical limits (i.e., greater than unity). Some temperature-dependent KIEs, however, show very large ΔE_a values that cannot be ascribed to mere isotopic differences in ZPE and, furthermore, show A_L/A_H values much lower than the semiclassical limit. For other reactions, A_L/A_H is close to unity and ΔE_a also falls within the semiclassical limits. Despite this large variation in the behavior of KIEs, the method described here provides excellent fits to the entire range of results, using either a single population (where possible) or two distinct populations. Among the systems examined here, we find a cutoff at a ΔE_a of ~ 1.5 kcal/mol (at 298 K) for H/T KIEs, above which a single conformational population cannot fit the KIEs (see the Supporting Information). Thus, as seen in Table 1, all of the systems where the H/T KIE exhibits a ΔE_a of >1 kcal/mol at 298 K can be fit only with the model that uses two populations. Thus, in those systems, the parameters in the single-population model are listed as not applicable (NA). Because the experimental data conform to a single-exponential function, two parameters are necessary and sufficient to describe the data. In the cases where $\Delta E_a = 0$ (within experimental error), the information content of the exper-

imental data reduces to a single parameter (A_L/A_H), so only a lower bound is given for the second fitting parameter in each model in Table 1. Truly temperature-independent KIEs imply no DAD sampling ($f = \infty$, or $\Delta G = \infty$), so the lower bound indicates the certainty (based on experimental errors) that the KIEs are truly temperature-independent; a larger lower bound means more certainty. It is important to note that different values of this lower bound report on the quality of the data analyzed rather than the nature of the system under study. One of the mutant enzymes in ref 14 (V108A) apparently exhibited inverse temperature dependence ($\Delta E_a < 0$), but the quality of the data and statistics are far from the quality of other data in the same work. Given the quality of these data and the fact that a negative ΔE_a could not be appropriately modeled by either one population or two populations, and because much higher levels of theory have examined only a few such cases,⁶⁸ we do not address these data here.

In general, the distributions we obtain using a single population for DHFR and its remote mutants agree qualitatively with QM/MM simulations that calculated the DAD PES for these enzymes,²⁶ suggesting that this kind of model truly captures the essential physics involved in H-transfer. Furthermore, in most cases, our fits agree with the trends found using nonadiabatic tunneling models.^{24,32} The fits to KIEs with little temperature dependence ($\Delta E_a < 1$ kcal/mol) show a correlation between ΔE_a and both the average DAD and the force constant of the corresponding harmonic potential (Table 1): a steep force constant and a short DAD give a small ΔE_a , while a longer DAD and a smaller force constant give a larger ΔE_a . Thus, in accordance with another recent analysis,³⁰ small force constants give smaller KIEs at higher temperatures because barrier compressions decrease rather than increase nuclear quantum effects. Barrier compression decreases the width and height of the barrier (Figure 4), allowing the isotopes to behave more similarly to one another. This behavior is consistent with the qualitative arguments that have emerged in recent years to describe these experimental results.^{1,8}

The observation that changes, such as mutations, alternate substrates, and nonphysiological temperature ranges, can change temperature-independent KIEs into temperature-dependent KIEs motivates the hypothesis that the conformational distribution along the DAD coordinate is important for enzyme-catalyzed reactions.^{14,24,26,38} In the context of small ΔE_a values, the DAD potential has a lower force constant and a longer average DAD.^{14,24,32,51} We cannot, however, model the steeply temperature-dependent KIEs ($\Delta E_a > 1$ kcal/mol at 298 K) with a single population and require at least two populations at the TRS. As with the one-population model, some clear trends emerge with respect to how the interplay between the two populations affects the temperature dependence of the KIEs with ΔE_a values of >1 kcal/mol (Table 1). If the DAD of the long population is especially long and much lower in energy, the system exhibits a larger ΔE_a .

The molecular interpretation of the two conformational substates for reactions with large ΔE_a values warrants further discussion. Perhaps the simplest interpretation of the models presented here comes in the context of the series of active-site mutants for *Escherichia coli* DHFR (Figure 8A). This set of experiments examined the effects of a hydrophobic residue in the active site (I14) that appears to hold the nicotinamide ring of the H-donor in place through steric effects.^{39,67} As the size of the residue decreases from I to V to A to G, ΔE_a becomes larger and larger. The wild type has a ΔE_a of ~ 0 , and thus, both

fitting models converge to a single, narrowly defined conformation with a DAD of 3.06 Å. At the other end of the series, the I14G mutant has a ΔE_a of 3.31 kcal/mol, and only the model with two populations can fit the data. One can interpret this as an indication that the missing side chain leaves so much space in the active site that the substrates can adopt different conformations, as also suggested by molecular dynamics (MD) studies.⁶⁷ The I14V and I14A mutants (ΔE_a values of 0.30 and 0.38 kcal/mol, respectively) can be modeled by either a single population or two populations. The results of a single population suggest that they have a smaller force constant and longer average DAD than the wild type; under the two-population model, they have a smaller ΔG and a shorter DAD_{long} than I14G. Because both models give adequate fits to these systems, these methods cannot indicate a preference for one interpretation over the other, and higher-level simulations will be necessary to make a judgment.

A closer examination of the differences between wild-type DHFR and its I14G mutant reveals how two distinct populations may lead to the steep temperature dependence of KIEs exhibited by the mutant (Table 1 and Figure 8A). In the mutant, the vast majority of the TRS population has a DAD long enough (3.33 Å) that the probability of H-tunneling is much larger than the probability for T (or D). A small portion of the population ($\approx 0.1\%$ at 298 K), however, is at a short enough DAD that all isotopes can cross the dividing surface between the reactant and product equally well. At low temperatures, a far greater overall population resides at the long DAD, where ¹H has a large advantage in tunneling, leading to a large KIE. An increasing temperature populates the short DAD (from which heavy isotopes can also be transferred), so the relative advantage of ¹H tunneling from the longer DAD decreases, resulting in strongly temperature-dependent KIEs. For the WT DHFR, on the other hand, a change in temperature will have the same effect on both isotopes: it will not cause a population shift, and the KIE change with temperature will be minimal.

The idea of a “steric hole” opening in the active site in the DHFR I14G mutant is a reasonable and intuitively satisfying explanation, but a similar interpretation of the conformational distributions of the G121V/M42W double mutant [residues distant from the active site (Figure 8B)], for example, seems less obvious. A limitation of this model is that it merely finds a one-dimensional distribution of DADs, without regard to other conformational fluctuations that may be important.⁴⁴ Thus, the distributions obtained represent ensembles of conformations, i.e., different states of “preorganization”.^{1,8}

The finding of distinct populations along the DAD coordinate is reminiscent of a recent suggestion that anomalously large Arrhenius pre-exponential factors in bsADH (and its mutants) result from the sampling of distinct conformations, each of which has different kinetic properties.⁶⁹ Additionally, pre-steady state experiments on a mutant of MR also suggested multiple kinetically distinct, reactive conformations and indicated that steady state rate measurements cannot probe the nature of such conformations.⁷⁰ Here we have shown that analysis of the temperature dependence of KIEs can uncover such reactive conformations, regardless of how the intrinsic KIEs were measured. Another recently published model of KIEs also suggested distinct reactive conformations.⁷¹ Like the two-conformation model presented here, the model by Mulholland and co-workers⁷¹ proposed one reactive conformation that proceeds by tunneling and one that surmounts

the barrier. Like that model, our two-state model for temperature-dependent KIEs does not depend on DAD fluctuations (only ΔG° between the states). This being said, nothing in the functional form of the model excludes the possibility of DAD fluctuations as we use for temperature-independent KIEs. A difficulty with that model, however, is that it requires nine parameters to describe data that fit to a single exponential (or two exponentials if the individual rates of the isotopes are considered). The model presented here, though, uniquely fits the temperature dependence of KIEs using just two fitting parameters.

CONCLUSIONS

We present a simple and user-friendly adiabatic model of H-tunneling in hydride- and proton-transfer reactions that can be used to generate a population distribution along the DAD coordinate by fitting to experimental KIEs and their temperature dependence. Practically, this new fit converts the isotope effect on entropy and enthalpy one gets from fitting to the Arrhenius or Eyring equations into two parameters indicative of the distribution of DADs. We suggest these two parameters provide a more molecular interpretation of the experimental data than ΔE_a and A_H/A_D . We demonstrate the utility of this fit for several enzymatic and nonenzymatic systems, including a number of different types of C–H → C transfers and other H-transfers. This simple, quantitative fitting of the experimental data, which is readily accessible to all experimentalists, gives a physically meaningful picture of how the temperature dependence of KIEs reflects the arrangement of the H-donor and H-acceptor. In the case of enzymatic reactions, this model provides parameters that correlate with the effects of mutations, alternative substrates, or changes in conditions that alter the ensemble of reactive conformations. For the nonenzymatic reactions, the parameters correlate with the rigidity of the reacting system, e.g., an intramolecular reaction in a fused ring system versus reactants with more conformational flexibility (see the Supporting Information). Importantly, the results imply that reactions with steeply temperature-dependent KIEs must occur from at least two distinct conformational substates: one that involves inefficient tunneling from a long DAD and one in which heavy-atom rearrangement (isotopically insensitive enzyme or solvent motion) brings the system to a short DAD where the ZPE of the transferred particle is above the barrier. In contrast to earlier phenomenological models, this procedure also reproduces small, steeply temperature-dependent KIEs (see the Supporting Information). Like previous phenomenological methods, the model presented here does not assume nonstatistical dynamic effects and uses the equilibrium distribution of DADs to calculate the tunneling probability. Because the model here that allows for multiple conformations can explain the full range of experimental data, while a single-population model cannot, this two-population model is more generally applicable. Of course, all the reactions studied here may occur from many different substates, and our model projects the full ensemble of substates onto two populations because the most one can extract from the given experimental data (KIEs and their temperature dependence) is two states, defined by two parameters. Additional experiments, as well as high-level calculations and simulations, will be necessary to determine more details of conformations that contribute to H-transfers for each specific system. This new tool is not meant to replace proper molecular calculations by QM/MM methods, but those techniques are expensive and highly specialized,

whereas this program is very simple to use and is available free of charge at <http://chemmath.chem.uiowa.edu/webMathematica/kohen/marcuslikemodel.html>.

■ ASSOCIATED CONTENT

■ Supporting Information

Additional discussion of the various systems analyzed by this computational model. This material is available free of charge via the Internet at <http://pubs.acs.org>.

■ AUTHOR INFORMATION

Corresponding Author

*E-mail: amnon-kohen@uiowa.edu. Phone: (319) 335-0234.

Funding

This work was supported by National Science Foundation (CHE-1149023), National Institutes of Health (NIH) (R01 GM65368), and United States-Israel Binational Science Foundation (2007256) grants to A.K. D.R. is supported by a predoctoral fellowship from the NIH (T32 GM008365).

Notes

The authors declare no competing financial interest.

■ ABBREVIATIONS

KIE, kinetic isotope effect; DAD, donor–acceptor distance; TST, transition state theory; TRS, tunneling-ready state; DHFR, dihydrofolate reductase; ADH, alcohol dehydrogenase; MR, morphinone reductase; PETNR, pentaerythritol tetranitrate; TSase, thymidylate synthase; PES, potential-energy surface; ZPE, zero-point energy; MD, molecular dynamics; QM/MM, quantum mechanics/molecular mechanics.

■ REFERENCES

- (1) Nagel, Z. D., and Klinman, J. P. (2010) Update 1 Of: Tunneling and Dynamics in Enzymatic Hydride Transfer. *Chem. Rev.* 110, PR41–PR67.
- (2) Hammes-Schiffer, S. (2006) Hydrogen Tunneling and Protein Motion in Enzyme Reactions. *Acc. Chem. Res.* 39, 93–100.
- (3) Truhlar, D. G. (2010) Tunneling in Enzymatic and Non-enzymatic Hydrogen Transfer Reactions. *J. Phys. Org. Chem.* 23, 660–676.
- (4) Warshel, A., Sharma, P. K., Kato, M., Xiang, Y., Liu, H. B., and Olsson, M. H. M. (2006) Electrostatic Basis for Enzyme Catalysis. *Chem. Rev.* 106, 3210–3235.
- (5) Schwartz, S. D. (2006) Vibrationally Enhanced Tunneling from the Temperature Dependence of Kie. In *Isotope Effects in Chemistry and Biology* (Kohen, A., and Limbach, H. H., Eds.) pp 475–498, Taylor & Francis, CRC Press, Boca Raton, FL.
- (6) Sen, A., and Kohen, A. (2010) Enzymatic Tunneling and Kinetic Isotope Effects: Chemistry at the Crossroads. *J. Phys. Org. Chem.* 23, 613–619.
- (7) Kiefer, P. M., and Hynes, J. T. (2006) Interpretation of Primary Kinetic Isotope Effects for Adiabatic and Nonadiabatic Proton-Transfer Reactions in a Polar Environment. In *Isotope Effects in Chemistry and Biology* (Kohen, A., and Limbach, H. H., Eds.) pp 549–578, Taylor & Francis, CRC Press, Boca Raton, FL.
- (8) Kohen, A. (2006) in *Isotope Effects in Chemistry and Biology* (Kohen, A., and Limbach, H.-H., Eds.) pp 743–764, Taylor & Francis, Boca Raton, FL.
- (9) Marcus, R. A. (2007) H and Other Transfers in Enzymes and in Solution: Theory and Computations, a Unified View. 2. Applications to Experiment and Computations. *J. Phys. Chem. B* 111, 6643–6654.
- (10) Bell, R. P. (1973) *The Proton in Chemistry*, 2nd ed., Cornell University Press, Ithaca, NY.

- (11) Kohen, A., Cannio, R., Bartolucci, S., and Klinman, J. P. (1999) Enzyme Dynamics and Hydrogen Tunneling in a Thermophilic Alcohol Dehydrogenase. *Nature* 399, 496–499.
- (12) Sikorski, R. S., Wang, L., Markham, K. A., Rajagopalan, P. T., Benkovic, S. J., and Kohen, A. (2004) Tunneling and Coupled Motion in the *Escherichia coli* Dihydrofolate Reductase Catalysis. *J. Am. Chem. Soc.* 126, 4778–4779.
- (13) Agrawal, N., Hong, B., Mihai, C., and Kohen, A. (2004) Vibrationally Enhanced Hydrogen Tunneling in the *E. coli* Thymidylate Synthase Catalyzed Reaction. *Biochemistry* 43, 1998–2006.
- (14) Pudney, C. R., Johannissen, L. O., Sutcliffe, M. J., Hay, S., and Scrutton, N. S. (2010) Direct Analysis of Donor Acceptor Distance and Relationship to Isotope Effects and the Force Constant for Barrier Compression in Enzymatic H-Tunneling Reactions. *J. Am. Chem. Soc.* 132, 11329–11335.
- (15) Pudney, C. R., Hay, S., Levy, C., Pang, J. Y., Sutcliffe, M. J., Leys, D., and Scrutton, N. S. (2009) Evidence to Support the Hypothesis That Promoting Vibrations Enhance the Rate of an Enzyme Catalyzed H-Tunneling Reaction. *J. Am. Chem. Soc.* 131, 17072–17073.
- (16) Fan, F., and Gadda, G. (2005) Oxygen- and Temperature-Dependent Kinetic Isotope Effects in Choline Oxidase: Correlating Reversible Hydride Transfer with Environmentally Enhanced Tunneling. *J. Am. Chem. Soc.* 127, 17954–17961.
- (17) Kwart, H., Brechbiel, M. W., Acheson, R. M., and Ward, D. C. (1982) Observations on the Geometry of Hydrogen Transfer in [1,5]Sigmatropic Rearrangements. *J. Am. Chem. Soc.* 104, 4671–4672.
- (18) Braun, J., Schwesinger, R., Williams, P. G., Morimoto, H., Wemmer, D. E., and Limbach, H. H. (1996) Kinetic H/D/T Isotope and Solid State Effects on the Tautomerism of the Conjugate Porphyrin Monoanion. *J. Am. Chem. Soc.* 118, 11101–11110.
- (19) Langer, U., Hoelger, C., Wehrle, B., Latanowicz, L., Vogel, E., and Limbach, H. H. (2000) ¹⁵N NMR Study of Proton Localization and Proton Transfer Thermodynamics and Kinetics in Polycrystalline Porphycene. *J. Phys. Org. Chem.* 13, 23–34.
- (20) Marcus, R. A., and Sutin, N. (1985) Electron Transfers in Chemistry and Biology. *Biochim. Biophys. Acta* 811, 265–322.
- (21) Kohen, A., Roston, D., Stojković, V., and Wang, Z. (2011) Kinetic Isotope Effects in Enzymes. In *Encyclopedia of Analytical Chemistry* (Meyers, R. A., Ed.) pp 77–99, John Wiley & Sons, Ltd., Chichester, U.K.
- (22) Hay, S., Sutcliffe, M. J., and Scrutton, N. S. (2009) Probing Coupled Motions in Enzymatic Hydrogen Tunneling Reactions: Beyond Temperature-Dependence Studies of Kinetic Isotope Effects. In *Quantum Tunneling in Enzyme-Catalysed Reactions* (Allemann, R. K., and Scrutton, N. S., Eds.) pp 199–218, Royal Society of Chemistry, Cambridge, U.K.
- (23) Kuznetsov, A. M., and Ulstrup, J. (1999) Proton and Hydrogen Atom Tunneling in Hydrolytic and Redox Enzyme Catalysis. *Can. J. Chem.* 77, 1085–1096.
- (24) Knapp, M. J., Rickert, K., and Klinman, J. P. (2002) Temperature-Dependent Isotope Effects in Soybean Lipoygenase-1: Correlating Hydrogen Tunneling with Protein Dynamics. *J. Am. Chem. Soc.* 124, 3865–3874.
- (25) Villa, J., and Warshel, A. (2001) Energetics and Dynamics of Enzymatic Reactions. *J. Phys. Chem. B* 105, 7887–7907.
- (26) Liu, H., and Warshel, A. (2007) Origin of the Temperature Dependence of Isotope Effects in Enzymatic Reactions: The Case of Dihydrofolate Reductase. *J. Phys. Chem. B* 111, 7852–7861.
- (27) Kiefer, P. M., and Hynes, J. T. (2004) Kinetic Isotope Effects for Nonadiabatic Proton Transfer Reactions in a Polar Environment. 1. Interpretation of Tunneling Kinetic Isotopic Effects. *J. Phys. Chem. A* 108, 11793–11808.
- (28) Borgis, D., and Hynes, J. T. (1996) Curve Crossing Formulation for Proton Transfer Reactions in Solution. *J. Phys. Chem.* 100, 1118–1128.
- (29) Kiefer, P. M., and Hynes, J. T. (2006) in *Isotope Effects in Chemistry and Biology* (Kohen, A., and Limbach, H.-H., Eds.) pp 549–578, Taylor & Francis, Boca Raton, FL.

- (30) Kamerlin, S. C. L., Mavri, J., and Warshel, A. (2010) Examining the Case for the Effect of Barrier Compression on Tunneling, Vibrationally Enhanced Catalysis, Catalytic Entropy and Related Issues. *FEBS Lett.* 584, 2759–2766.
- (31) Please note that enzymes only evolve for H-transfer (rather than D- or T-transfers), and although many WT enzymes exhibit temperature-independent KIEs, this result does not necessarily indicate a faster reaction rate (ref 15) or otherwise better evolved enzyme.
- (32) Meyer, M. P., and Klinman, J. P. (2005) Modeling Temperature Dependent Kinetic Isotope Effects for Hydrogen Transfer in a Series of Soybean Lipoygenase Mutants: The Effect of Anharmonicity Upon Transfer Distance. *Chem. Phys.* 319, 283–296.
- (33) Hatcher, E., Soudackov, A. V., and Hammes-Schiffer, S. (2007) Proton-Coupled Electron Transfer in Soybean Lipoygenase: Dynamical Behavior and Temperature Dependence of Kinetic Isotope Effects. *J. Am. Chem. Soc.* 129, 187–196.
- (34) Pu, J., Ma, S., Gao, J., and Truhlar, D. G. (2005) Small Temperature Dependence of the Kinetic Isotope Effect for the Hydride Transfer Reaction Catalyzed by *Escherichia coli* Dihydrofolate Reductase. *J. Phys. Chem. B* 109, 8551–8556.
- (35) Kanaan, N., Ferrer, S., Martin, S., Garcia-Viloca, M., Kohen, A., and Moliner, V. (2011) Temperature Dependence of the Kinetic Isotope Effects in Thymidylate Synthase. A Theoretical Study. *J. Am. Chem. Soc.* 133, 6692–6702.
- (36) Wang, L., Tharp, S., Selzer, T., Benkovic, S. J., and Kohen, A. (2006) Effects of a Distal Mutation on Active Site Chemistry. *Biochemistry* 45, 1383–1392.
- (37) Wang, L., Goodey, N. M., Benkovic, S. J., and Kohen, A. (2006) The Role of Enzyme Dynamics and Tunneling in Catalyzing Hydride Transfer: Studies of Distal Mutants of Dihydrofolate Reductase. *Philos. Trans. R. Soc. London, Ser. B* 361, 1307–1315.
- (38) Wang, L., Goodey, N. M., Benkovic, S. J., and Kohen, A. (2006) Coordinated Effects of Distal Mutations on Environmentally Coupled Tunneling in Dihydrofolate Reductase. *Proc. Natl. Acad. Sci. U.S.A.* 103, 15753–15758.
- (39) Stojkovic, V., Perissinotti, L. L., Lee, J., Benkovic, S. J., and Kohen, A. (2010) The Effect of Active-Site Isoleucine to Alanine Mutation on the DHFR Catalyzed Hydride-Transfer. *Chem. Commun.* 46, 8974–8976.
- (40) Wang, Z., and Kohen, A. (2010) Thymidylate Synthase Catalyzed H-Transfers: Two Chapters in One Tale. *J. Am. Chem. Soc.* 132, 9820–9825.
- (41) Nagel, Z. D., Meadows, C. W., Dong, M., Bahnson, B. J., and Klinman, J. P. (2012) Active Site Hydrophobic Residues Impact Hydrogen Tunneling Differently in a Thermophilic Alcohol Dehydrogenase at Optimal Versus Nonoptimal Temperatures. *Biochemistry* 51, 4147–4156.
- (42) Bandaria, J. N., Cheatum, C. M., and Kohen, A. (2009) Examination of Enzymatic H-Tunneling through Kinetics and Dynamics. *J. Am. Chem. Soc.* 131, 10151–10155.
- (43) Roth, W. R., and Konig, J. (1966) Wasserstoffverschiebungen. 4. Kinetischer Isotopeneffekt Der 1.5-Wasserstoffverschiebung Im Cis-Pentadien-(1.3). *Ann. Chem.* 699, 24–32.
- (44) Brooks, C. L., and Thorpe, I. F. (2005) Conformational Substates Modulate Hydride Transfer in Dihydrofolate Reductase. *J. Am. Chem. Soc.* 127, 12997–13006.
- (45) Alhambra, C., Corchado, J. C., Sanchez, M. L., Gao, J. L., and Truhlar, D. G. (2000) Quantum Dynamics of Hydride Transfer in Enzyme Catalysis. *J. Am. Chem. Soc.* 122, 8197–8203.
- (46) Agarwal, P. K., Webb, S. P., and Hammes-Schiffer, S. (2000) Computational Studies of the Mechanism for Proton and Hydride Transfer in Liver Alcohol Dehydrogenase. *J. Am. Chem. Soc.* 122, 4803–4812.
- (47) Cui, Q., Elstner, M., and Karplus, M. (2002) A Theoretical Analysis of the Proton and Hydride Transfer in Liver Alcohol Dehydrogenase (LADH). *J. Phys. Chem. B* 106, 2721–2740.
- (48) Major, D. T., Heroux, A., Orville, A. M., Valley, M. P., Fitzpatrick, P. F., and Gao, J. (2009) Differential Quantum Tunneling Contributions in Nitroalkane Oxidase Catalyzed and the Uncatalyzed Proton Transfer Reaction. *Proc. Natl. Acad. Sci. U.S.A.* 106, 20734–20739.
- (49) Frisch, M. J., Trucks, G. W., Schlegel, H. B., Scuseria, G. E., Robb, M. A., Cheeseman, J. R., Montgomery, J. A., Jr., Vreven, T., Kudin, K. N., Burant, J. C., Millam, J. M., Iyengar, S. S., Tomasi, J., Barone, V., Mennucci, B., Cossi, M., Scalmani, G., Rega, N., Petersson, G. A., Nakatsuji, H., Hada, M., Ehara, M., Toyota, K., Fukuda, R., Hasegawa, J., Ishida, M., Nakajima, T., Honda, Y., Kitao, O., Nakai, H., Klene, M., Li, X., Knox, J. E., Hratchian, H. P., Cross, J. B., Bakken, V., Adamo, C., Jaramillo, J., Gomperts, R., Stratmann, R. E., Yazyev, O., Austin, A. J., Cammi, R., Pomelli, C., Ochterski, J. W., Ayala, P. Y., Morokuma, K., Voth, G. A., Salvador, P., Dannenberg, J. J., Zakrzewski, V. G., Dapprich, S., Daniels, A. D., Strain, M. C., Farkas, O., Malick, D. K., Rabuck, A. D., Raghavachari, K., Foresman, J. B., Ortiz, J. V., Cui, Q., Baboul, A. G., Clifford, S., Cioslowski, J., Stefanov, B. B., Liu, G., Liashenko, A., Piskorz, P., Komaromi, I., Martin, R. L., Fox, D. J., Keith, T., Al-Laham, M. A., Peng, C. Y., Nanayakkara, A., Challacombe, M., Gill, P. M. W., Johnson, B., Chen, W., Wong, M. W., Gonzalez, C., and Pople, J. A. (2004) *Gaussian 03*, revision E.01, Gaussian, Inc., Wallingford, CT.
- (50) Wolfram Research, Inc. (2008) *Mathematica*, version 7.0, Wolfram Research, Inc., Champaign, IL.
- (51) Hay, S., Sutcliffe, M. J., and Scrutton, N. S. (2007) Promoting Motions in Enzyme Catalysis Probed by Pressure Studies of Kinetic Isotope Effects. *Proc. Natl. Acad. Sci. U.S.A.* 104, 507–512.
- (52) Warshel, A., and Chu, Z. T. (1990) Quantum Corrections for Rate Constants of Diabatic and Adiabatic Reactions in Solutions. *J. Chem. Phys.* 93, 4003–4015.
- (53) Kim, Y., Truhlar, D. G., and Kreevoy, M. M. (1991) An Experimentally Based Family of Potential-Energy Surfaces for Hydride Transfer between NAD⁺ Analogs. *J. Am. Chem. Soc.* 113, 7837–7847.
- (54) Roston, D., and Kohen, A. (2010) Elusive Transition State of Alcohol Dehydrogenase Unveiled. *Proc. Natl. Acad. Sci. U.S.A.* 107, 9572–9577.
- (55) Cohen-Tannoudji, C., Diu, B., and Laloë, F. (1977) *Quantum Mechanics*, Wiley, New York.
- (56) Kiefer, P. M., and Hynes, J. T. (2003) Kinetic Isotope Effects for Adiabatic Proton Transfer Reactions in a Polar Environment. *J. Phys. Chem. A* 107, 9022–9039.
- (57) de la Lande, A., Rezac, J., Levy, B., Sanders, B. C., and Salahub, D. R. (2011) Transmission Coefficients for Chemical Reactions with Multiple States: Role of Quantum Decoherence. *J. Am. Chem. Soc.* 133, 3883–3894.
- (58) Borgis, D. C., Lee, S. Y., and Hynes, J. T. (1989) A Dynamical Theory of Nonadiabatic Proton and Hydrogen-Atom Transfer-Reaction Rates in Solution. *Chem. Phys. Lett.* 162, 19–26.
- (59) Ohta, Y., Soudackov, A. V., and Hammes-Schiffer, S. (2006) Extended Spin-Boson Model for Nonadiabatic Hydrogen Tunneling in the Condensed Phase. *J. Chem. Phys.* 125, 144522–144537.
- (60) Hwang, J. K., King, G., Creighton, S., and Warshel, A. (1988) Simulation of Free-Energy Relationships and Dynamics of sn2 Reactions in Aqueous-Solution. *J. Am. Chem. Soc.* 110, 5297–5311.
- (61) Olsson, M. H. M., Parson, W. W., and Warshel, A. (2006) Dynamical Contributions to Enzyme Catalysis: Critical Tests of a Popular Hypothesis. *Chem. Rev.* 106, 1737–1756.
- (62) Alhambra, C., Corchado, J., Sanchez, M. L., Garcia-Viloca, M., Gao, J., and Truhlar, D. G. (2001) Canonical Variational Theory for Enzyme Kinetics with the Protein Mean Force and Multidimensional Quantum Mechanical Tunneling Dynamics. Theory and Application to Liver Alcohol Dehydrogenase. *J. Phys. Chem. B* 105, 11326–11340.
- (63) Agarwal, P. K., Billeter, S. R., and Hammes-Schiffer, S. (2002) Nuclear Quantum Effects and Enzyme Dynamics in Dihydrofolate Reductase Catalysis. *J. Phys. Chem. B* 106, 3283–3293.
- (64) Olsson, M. H. M., Mavri, J., and Warshel, A. (2006) Transition State Theory Can Be Used in Studies of Enzyme Catalysis: Lessons from Simulations of Tunneling and Dynamical Effects in Lipoygenase and Other Systems. *Philos. Trans. R. Soc. London, Ser. B* 361, 1417–1432.

- (65) Warshel, A. (1982) Dynamics of Reactions in Polar-Solvents: Semi-Classical Trajectory Studies of Electron-Transfer and Proton-Transfer Reactions. *J. Phys. Chem.* 86, 2218–2224.
- (66) Warshel, A. (1984) Dynamics of Enzymatic-Reactions. *Proc. Natl. Acad. Sci. U.S.A.* 81, 444–448.
- (67) Stojkovic, V., Perissinotti, L. L., Willmer, D., Benkovic, S. J., and Kohen, A. (2012) Effects of the Donor-Acceptor Distance and Dynamics on Hydride Tunneling in the Dihydrofolate Reductase Catalyzed Reaction. *J. Am. Chem. Soc.* 134, 1738–1745.
- (68) Ludlow, M. K., Soudackov, A. V., and Hammes-Schiffer, S. (2009) Theoretical Analysis of the Unusual Temperature Dependence of the Kinetic Isotope Effect in Quinol Oxidation. *J. Am. Chem. Soc.* 131, 7094–7102.
- (69) Nagel, Z. D., Dong, M., Bahnson, B. J., and Klinman, J. P. (2011) Impaired Protein Conformational Landscapes as Revealed in Anomalous Arrhenius Prefactors. *Proc. Natl. Acad. Sci. U.S.A.* 108, 10520–10525.
- (70) Pudney, C. R., Hay, S., Pang, J. Y., Costello, C., Leys, D., Sutcliffe, M. J., and Scrutton, N. S. (2007) Mutagenesis of Morphinone Reductase Induces Multiple Reactive Configurations and Identifies Potential Ambiguity in Kinetic Analysis of Enzyme Tunneling Mechanisms. *J. Am. Chem. Soc.* 129, 13949–13956.
- (71) Glowacki, D. R., Harvey, J. N., and Mulholland, A. J. (2012) Taking Ockham's Razor to Enzyme Dynamics and Catalysis. *Nat. Chem.* 4, 169–176.